Modular Volumetric Actuators Using Motorized Auxetics

Jeffrey Lipton[1,2], Lillian Chin[1], Jacob Miske[1], and Daniela Rus[1]

Abstract— **Volume change has become a critical actuation method in robotics. However, the need for fluid flow or thermal processes to generate volume changes limits the durability, speed, and efficiency of these actuators. In this paper, we develop a new electromechanical actuator that volumetrically expands. By combining auxetic materials with a servo, we produce a simple isotropically expanding actuator that can be modularly composed. We discuss the symmetry considerations in selecting an appropriate auxetic framework for our actuator, eventually choosing a double-layered polyhedral auxetic design. Characterization shows that a single actuator can expand in radius to 119% of the original size and generate 90N of force, while maintaining a small package and a speedy expansion / contraction cycle. Finally, we demonstrate the modularity of our actuators by linking three actuators to create a vertical tube-crawling robot. The small package and fast cycle time of our system highlight how viable these electromechanical volumetric actuators can be as an important actuator modality.**

I. INTRODUCTION

Independent cellular volumetric actuation has the potential to solve many of the issues traditionally associated with soft robots. Soft robotics has in large part relied on open-cell fluid-driven volumetric actuation, where volumes of fluid are moved between a reservoir and a series of open cells. This has been used to great success in diverse fluidic mediums such as air, vacuum, and water [1–3].

However, these open-cell designs introduce a significant weaknesses into soft robotics: susceptibility to puncture. The interconnected nature of these systems means that if any of these open cells were to be punctured, the puncture would cascade down the entire actuation system and cause it to fail. Despite the significant amount of work on making self-healing and puncture resistant soft robots [4, 5], these efforts do not address the underlying issue of having a single point of failure across distributed fluid chambers.

Bioinsipiration offers a solution to this cascading failure issue: independent cellular volumetric actuation. By having isolated cells, a failure at one point does not cause the entire system to fail. Indeed, plants and several animals use differentially change the volume of their cells in order to move – a process known as auxesis [6, 7]. Auxesis has been replicated in simulation through evolutionary algorithims, demonstrating the potential of independently size-changing cells as an actuator [8–10]. Past attempts at making independent cellular volumetric actuators for soft robots have relied on thermally induced phase changes, resulting in slow

[1]Computer Science and Artificial Intelligence Lab, MIT, 32 Vassar Street, Cambridge, MA, 02139, USA email: {jlipton, ltchin, miske, rus}@csail.mit.edu

[2] Mechanical Engineering Department, University of Washington, Seattle, WA, USA.

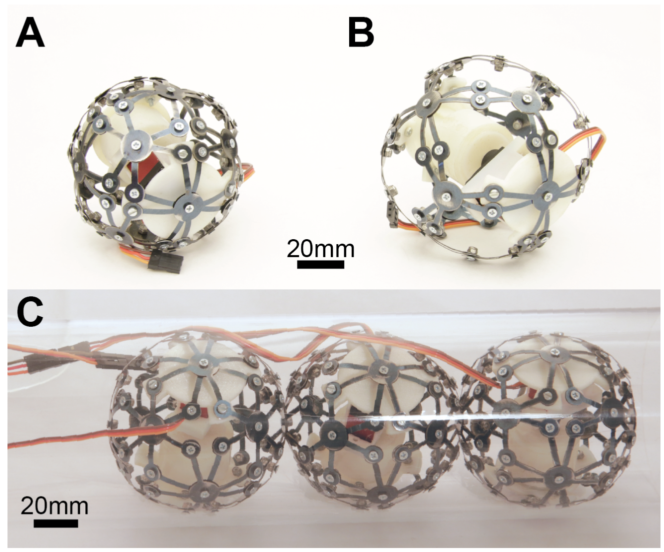

Fig. 1. Overview of electric volumetric actuator in (A) closed state and (B) fully actuated open state. These actuators can be combined modularly in order to build more complex robots, such as (C) a peristaltic tube crawler.

actuators [11, 12]. As a result, attempts to realize these evolved soft robots have thus far been hindered by the lack of reliable and responsive hardware equivalents.

To address these challenges, we have developed an electromechanical volumetric actuator that can be composed modularly into independent cells (Fig. 1). We emulate the cellular expansion / auxesis found in nature by combining standard servos with auxetic materials. Auxetic materials are cellular materials that expand across all perpendicular directions simultaneously (i.e. materials with a negative Poisson's ratio). Each single actuator is made up of an auxetic skeleton and an internal core that translates a servo's rotational movements into the shell's volumetric expansion.

We explore the space of auxetic symmetries to decide and fabricate an appropriate shell design, building a final actuator capable of generating 90 N of force and expanding to 119% of its original size. These shells provide the structure with an effective modulus of 76 kPa. This places these actuators in the realm of soft robotics, as it is significantly less than the stiffness of the commonly used Smooth-On Dragon Skin 30 elastomeric silicone (593 kPa) [?]. This actuator's small package, modularity, and moderate compliance allows us to build a simple tube crawling robot more easily than standard fluidic methods and without the fear of cascading failure.

In this paper we:

- determine the ideal families of auxetic structures for volumetric actuators

- develop and characterize an auxetic volumetric actuator
- demonstrate the actuator's utility and modularity by making a tube crawling robot

II. BACKGROUND

A. Closed-cell Volumetric Actuators

Although most current soft robotics efforts have focused on open-cell designs, early work actually relied on using closed-cell foams as actuators [8]. These actuators responded to a cyclic change in external pressure. While obviously not useful outside of a pressure chamber, they did demonstrate the potential for soft cellular actuation.

More recent work on closed-cell volumetric actuators has relied on changing the state of matter in the cell, primarily through electrically driven phase changes. By inducing boiling or melting in a material, these actuators can undergo dramatic expansion or generate extremely high forces [11–13]. Their closed cell nature also allows them to be extremely resilient. Electrically actuated hydraulic solids, for example, can be cut in half or punctured, and still generate up to 4.5 kN of force [11]. While impressive, the thermal nature of their actuation means that all of these closed-cell actuators can either only be actuated once or have a very slow cycle time.

B. Expanding Modular Robots

This paper builds not only off of volumetric actuators in the soft robotic community, but also off of the modular robotics community. Expanding and contracting unit cells have been shown to be useful for group movement, especially in an expanding lattice formation. Crystalline atom robots were inspired by muscles' and amoebas' expansion / contraction movements to move collectively across the plane. Each robot had only one degree of freedom through a rack and pinion mechanism, but could work together to reconfigure themselves to generic shapes [14]. Telecubes extended this concept to 3D by having a set of cubes that could extend each of their faces independently from a central core, allowing cubes to magnetically slide past one another to reconfigure [15]. Both of these demonstrated the power of expanding/contracting unit cells. Crystalline atom robots demonstrate the potential for auxetic actuation, but only in the plane, and Telecubes demonstrated the utility of volumetric expansion, but had overly complex actuation mechanisms.

C. Auxetics in Robotics

Auxetic materials have been a useful tool in the soft robotics toolkit, primarily in conjunction with pneumatic actuation. While they have been used as soft passive elements in penumatic systems [16, 17], auxetic cells are more commonly connected to a single vacuum channel, which is then used to induce buckling/contraction in the overall structure [18, 19]. In 2D, if this technique is used to make two or more counter-rotating sections, grippers, linear actuators and locomoting robots can be created [20, 21]. When this 2D pattern is tiled around a sphere, a true 3D volumetric actuator can be created [18]. All of these techniques, however, have the same standard drawbacks that come with relying on fluidic systems.

An exception to this pneumatic integration pattern has been handed shearing auxetic cylinders [22]. These structures directly convert the rotation of a motor into a linear and radial expansion. Constraints on the linear actuation can then be used to produced curved bending for grippers [23]. While these actuators do expand in volume, they are primarily linear actuators and not suitable for the independent closed cell actuation we desire.

III. AUXETIC ACTUATOR DESIGN

In order to create an auxetic and electromechanical volumetric actuator, we need a way to integrate an auxetic design with a motor to induce expansion. We do so by designing an auxetic shell driven by an internal motor core, creating an independent cell. Our design process must thus answer the following questions:

1) What possible auxetic designs will lead to volumetric expansion?
2) Which auxetic design is the most appropriate for our application?
3) How will the internal motor core induce expansion?

A. Auxetic Shell Symmetries

To understand how to design an auxetic pattern that leads to volumetric expansion, we must understand the group theory behind auxetic materials, as elaborated in [22].

1) Potential Auxetic Designs: Auxetic materials can be represented as single degree-of-freedom bars-and-joints frameworks describing repeated unit cells that tile the plane or space. These unit cells can be composed of links, polygons or a combination of the two, but must contain a single degree-of-freedom, θ, an angle between two bars. As θ varies from a minimum to maximum value, the overall unit cell tessellation will change shape, causing an "auxetic trajectory". Fig. 2 demonstrates how a change in θ causes the overall shape to travel an auxetic trajectory. As the angle between the unit cell's elements changes, the sphere expands, reaches a maximum extent, and then retracts.

Since the unit cell must tile the plane/space, the unit cell must satisfy certain constraints on its symmetries. For 3D auxetics, like our volumetric actuator, the unit cell must belong to one of the 230 space groups, each of which has a point group basis. These point groups represent the symmetries of the surface of a sphere and can be one of seven families of axial groups or one of the seven polyhedral groups. For our volumetric actuator, we need our auxetic shell to have symmetries in one of the point groups.

This provides us with our first design choice: axial symmetry or polyhedral symmetry. Axial symmetries take the sphere and orient it, selecting two antipodal points as the poles of the sphere and defining an equator for the sphere. The shearing auxetics described in [22] and seen in Fig. 2A are examples of auxetics that are part of the axial symmetry groups. The sphere itself has a four way symmetry at the

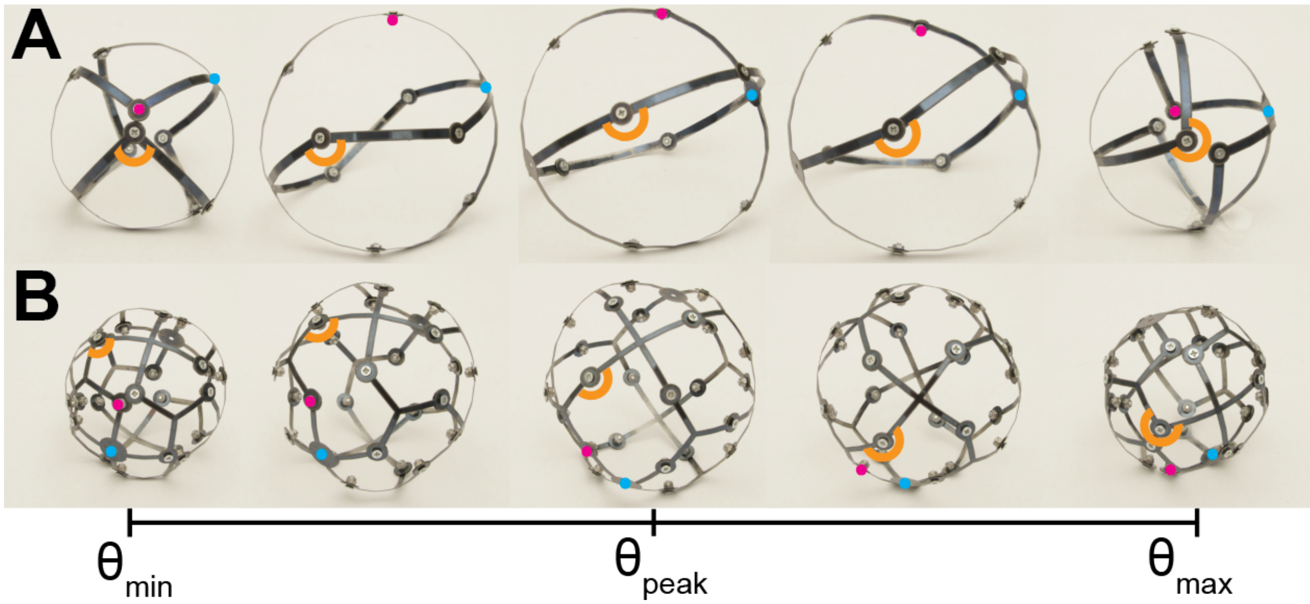

Fig. 2. Open-close trajectories for proposed single-layer skeletons of the point actuators. Both the (A) axial auxetics and the (B) polyhedral auxetics exhibit a twist to open, as can be seen by the change in angle indicated in orange from θ_{min} to θ_{max}, with maximum open size at θ_{peak}. Pink and blue dots have been added to more easily track the movement of the auxetic skeleton.

poles, but, in theory, could be made with an infinite number of bars reaching between the poles. In practice, the thickness of the links limits the symmetries around the poles.

Additionally, since we wish to turn the rotation of a motor into the expansion of the auxetic framework, we want at least one set of antipodal points to rotate relative to each other as the auxetic framework moves along its auxetic trajectory. Not all point group auxetics exhibit this behavior. The famous Hoberman sphere [24], for example, has icosahedral symmetry, but does not have any rotation between antipodal points. As a result, the Hoberman Sphere would need to be driven by rotations at the joints or with a linear actuator. While it is possible to make cells this way, it increases the complexity and relative size of the mechanism.

While many polyhedral symmetric patterns are eliminated by the antipodal rotation requirement, the five rotating polyhedral patterns described in [18] satisfy this condition. These five patterns, like all polyhedral symmetric patterns, do not orient the sphere – defining no poles or equator.

Fig. 2B demonstrates an auxetic that is part of the polyhedral symmetry group. The auxetic pattern in Fig. 2B consist of squares and triangles rotating relative to each other. The spring steel frame of the structure represents these polygons by having struts connect the polygons' centers to their respective corners, creating a Y-shape for the triangles and an X-shape for the squares. This eliminates unnecessary material while maintaining the kinematics of the frame, as we see the pattern in Fig. 2B transition between a cuboctahedron in the collapsed state, and a rhombicuboctahedron in the open state.

2) Selecting a Symmetry Group: Although both the shearing axial and the rotating polyhedral patterns satisfy the requirement of point group symmetry and antipodal rotation, they do not have the same trade offs. The shearing axial auxetics can generate much larger expansions than the polyhedral patterns. While the pattern shown in Fig. 2A has only a slightly larger expansion relative to the polyhedral auxetic in Fig. 2B, shearing axial patterns can have a radial expansion of up to 2.5 times [22], while polyhedral patterns generally have a maximum expansion around 1.7 times [25].

However, the axial patterns from [22] are much weaker than the polyhedral patterns. The axial patterns have no cross bracing around the equator, so any loading along the equator is poorly supported. By contrast, the polyhedral patterns are isotropic in stiffness; by not being oriented, there is no preferred loading direction. The axial patterns also have more energy stored in the frame during expansion, causing its bars to bend and change radius as the pattern expands. This causes energy to be converted from expansion to stress in the frame, weakening the overall structure for a higher required force. The polyhedral design, by contrast, consists of beams that only rotate relative to each other and never bend during expansion, reducing stress in the overall frame. One must conclude that polyhedral frames are preferable to the shearing axial frame designs for the reasons listed above.

B. Auxetic Shell Design and Fabrication

From the previous section, we knew that our volumetric actuator will be a polyhedral auxetic pattern. We chose the pattern from Fig. 2B as the polyhedral shell because it was the simplest pattern that provided centers along the three perpendicular directions, allowing for cubic tiling.

We further noted that we have the ability to integrate a second layer of this polyhedral auxetic pattern into a single shell. As seen in Fig. 2B, this polyhedral pattern has a symmetric auxetic trajectory. It starts in a compact state, expands to a maximum, and then collapses to another compact state. Therefore, for each point along the auxetic trajectory, there is a point that is its mirror image. If one were to composite these mirrored points on top of each other, the structure would gain mirror symmetries. For polyhedral patterns, the centers of the polyhedra can be connected and aligned between the layers.

We decided to use a double layer shell for the actuator because we believed it would provide a more robust framework with improvements to the stiffness of the structures. Rather than build the double shell as two separate layers placed on top of each other, we interdigitated the two copies of the polyhedral shell from Fig. 2B. into an integrated double layer shell, as seen in Fig. 1A and B. In other words, one pattern had the square sections on top and the triangles on the bottom, while the other layer had the triangles on top and the squares on the bottom. This arrangement ensured the smoothest structure with minimal friction caused by the forced overlap caused by joining the two polygons layers together.

While in theory, a double layered shell can have the same exact range of motion as the single layer shell, in practice, this is not the case. As seen in Fig. 1A and B, the thickness of the bars and joints limits the ability of the shell to fully contract and fulled expand. The limitation on the auxetic trajectory range has the effect of eliminating the point of maximal expansion. As a result, the double shell cannot twist from compact to extended to compact again with a monotonically increasing or decreasing θ. Instead, θ is limited to increase to expand, and decrease to contract. A downside of the double layer design results from the elimination of the point of maximal extension. At that point, extension enters a singularity and extension and compression cannot cause the bar-and-joint framework to rotate to expand and contract.

The frames of the final double-layer actuators were made from 0.254 mm thick spring steel cut on a waterjet. The joints were made from 2 mm screws with nylon lock nuts. The bars on the shearing auxetic frames are 4 mm wide, and the struts for the polyhedral frame were 2.5 mm wide. The shearing auxetic frames were pre-bent around a 65 mm diameter template. The polyhedral frame was bend at the transition from the bar to the joint and from the center to the joint and made to fit the 65 mm diameter template. The frames for the single layer version had no holes in the center, while the frames for the double layer structure had holes in the center of the frames. The circle surrounding the central hole was 12.75 mm in diameter.

C. Motorizing the Shell

In order to motorize the shell, we need to connect the motor to the antipodal points on the shell without over-constraining the device. This is because the shell inherently connects rotation of antipodal points to expansion, allowing us to just use a simple twist to expand the shell. Since the double layered, polyhedral auxetic structure has a handed behavior, there is only one way to twist the structure open, and we do not need to worry about constraining a single handed direction. Furthermore, we can use a standard servo motor as the rotation between antipodal points is limited to less than 90 degrees, we can use a standard servo motor.

Inside the frame, a servo (Power HD Mini Digital Servo HD-1810MG) is attached to a 3D printed internal support (VeroWhite, Objet Connex 260). The internal support is attached to the corners of one of the square polygons as a mounting point, leaving space between the center of the polygon and the support.

We then use a 3D-printed collapsible column to connect the servo horn to the opposite side of the shell. This column consists of two structures: a ring with 4 small roller bearings (3/32” x 3/16” x 3/32”, AVID) attached to the servo horn, and support structure with tracks. The support structure with tracks is connected to a square polygon in the same manner as the motor support. This bearing and linear track system thus couples the rotation of the servo to the rotation of the antipodal points. This keeps the shell unconstrained, allowing the shell to entirely drive the extension of the internal column.

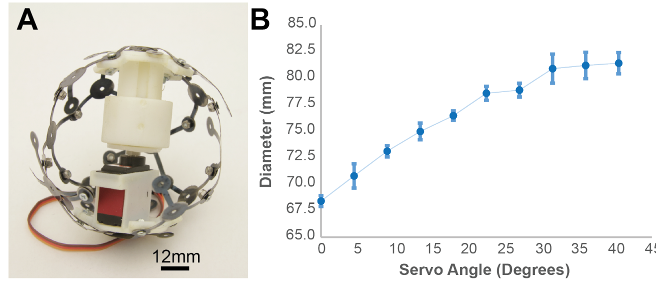

Fig. 3. (A) Internal motor and piston system for the polyhedral auxetic actuator. Since twisting is coupled with extension, inducing an unconstrained twist cause the entire system to expand. (B) We characterize the integrated double-layer actuator by comparing servo angle to actuator diameter.

TABLE I
PROPERTIES OF DOUBLE-LAYER POLYHEDRAL AUXETIC ACTUATOR

Weight	80 ± 3 g
Closed Diameter	68.4 ± 0.5 mm
Open Diameter	81.4 ± 1 mm
Maximum Expansion Rate	26 mm/s
Minimum Cycle Time	500 ms
Maximum Top Load	90 N
Top-Loaded Stiffness	4900 ± 280 N/m
Top-Loaded Blocked Force	5.9 ± 0.2 N
Maximum Lateral Load	32 N
Lateral-Loaded Stiffness	1800 ± 240 N/m
Lateral-Loaded Blocked Force	4.7 ± 0.1 N

IV. SINGLE ACTUATOR CHARACTERIZATION

We proceed by characterizing the performance of a single volumetric actuator in order to understand its performance when assembled as part of a unit of a more complex robot.

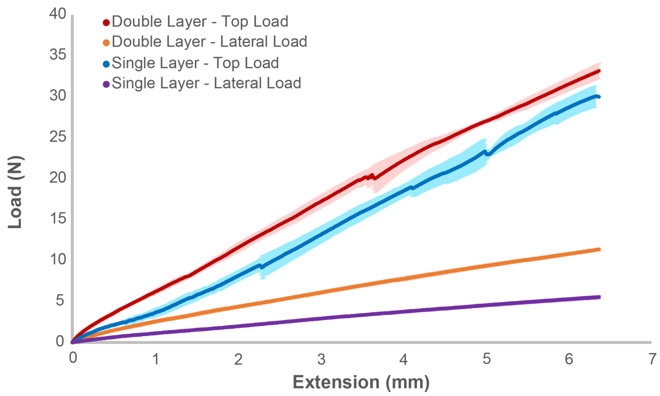

Fig. 4. Compression tests of both single and double layer polyhedral auxetic actuators under top and lateral loading for small deformations in the linear regime. Under both loading conditions, the double layer auxetic performed better than the single layer version, demonstrating nearly twice as much stiffness than the single layer under lateral loading.

The results of these experiments are summarized in Table I.

Weights were measured for 3 different units using a standard high precision scale with milligram accuracy. Diameters were measured using digital calipers with 100 micron accuracy. We subjected a single unit in an expanded state to destructive testing of for maximal load on lateral and a different one to top loaded conditions. We measured the blocked force of the actuator by placing a closed cell in an Instron with a $2kN$ load-cell and powered the servo without moving the head of the Instron. To determine the maximal load of the linear region a single unit was compressed to failure for both the lateral and top loading conditions. The end of the linear region is reported as the maximum load for the condition.

To confirm our assumptions about choosing a double layer design over a single layer design, we conducted a compression test for both systems under top loading conditions (aligned with the servo) and lateral loading conditions (orthogonal to the servo). As can be seen in Fig. 4, over three trials, both designs fared about the same under top loading, but the double layer design was about twice as stiff as the single layer design under lateral loading. This confirms our intuition that adopting a double layer would help better simulate an isotropic material.

Our double layer design increases in diameter from 68.4 ± 0.5 mm to 81.4 ± 1 mm, a 1.19 times increase in size. This is significantly smaller than the typical expansion factor of polyhedral auxetics which is a 1.5 times increase. We suspect that this is due to the passive nature of our untwisting mechanism. Since we rely on an unconstrained twist to induce expansion, any friction between the spring steel at the pin joints can prevent the structure actuating to its fullest extent. Furthermore, due to the second layer, interference between the screws at the pin joints can also prevent completely achieving a compact form.

To quantify the rate of expansion and speed of actuation, we conducted open-close cycle tests, gradually increasing the motor speed until we judged that the unit cell was no longer opening and closing fully, or a part became damaged. We found that the fastest our system was able to reliably complete an open-close cycle was 500 ms, corresponding to a radial expansion of 26 mm/s. This is significantly faster than other volumetric actuators, especially those that rely on a cool down time to reset. However the servos have a no-load speed of 8 rad/s, which would cycle in 200 μs so faster cycling without load should be possible.

In both the compression test and the expansion rate test, the point of failure was always the internal plastic mechanism cracking, rather than the motor. This is promising, as this shows that our design is not limited in strength by amount of actuation needed to move the system, but by the strength of our individual components. Replacing the internal 3D printed mechanism with stronger materials like milled metal or injection-molded plastic could improve the performance of our volumetric actuator significantly.

V. MULTI-UNIT EVALUATION

A. Peristaltic Crawler Design

In order to compare the utility of these electromechanical auxetic cells to previous fluid-driven auxetic soft robots, we built a tube crawler and compare it to the reported metrics of [16], a pneumatic-auxetic hybrid tube crawler.

Each of our actuators can be thought of as a single unit cell for more complex robots, coupling to one another at the center of polyhedral faces like a cubic lattice. To make our tube crawler, we connected three auxetic cells together in a line orthogonal to the servo column. We then placed the crawler in a constraining tube with a diameter of 82.4 mm, slightly less than that of the fully expanded cell.

Unlike [16], our crawler robot used peristaltic motion to move through the robot. To inch along the tube, the robot goes through a series of seven steps, successively opening and closing cells in a predefined motion (Fig. 5). In order for the entire bot to avoid slipping in the tube, one bot must be able to stay in place while the other two bots expand. By alternating which cells are closed, a mechanical wave travels through the robot, allowing for net motion.

B. Evaluation

In order to evaluate the robot, we tested the system in a horizontal and vertical tube crawl and measured its speed. Each actuator ran with a open-close cycle time of 1 s, twice as long as the estimated maximum cycle speed, to reduce chance of the 3D printed internal structures from breaking.

In a horizontal crawling test, the crawler moved 38.1 mm in one minute, representing a speed of 0.031 body-lengths per second. In a vertical crawling test, the three bot structure moved slower at 15.24mm in one minute, representing a speed of 0.012 body lengths per second.

The discrepancy in speed between the vertical and horizontal tube crawl is due to slippage between the cells and the tube. Both of these speeds, however, are slower than the 0.08 body-lengths per second reported in [16], even accounting for halving our speed to prevent internal supports from breaking.

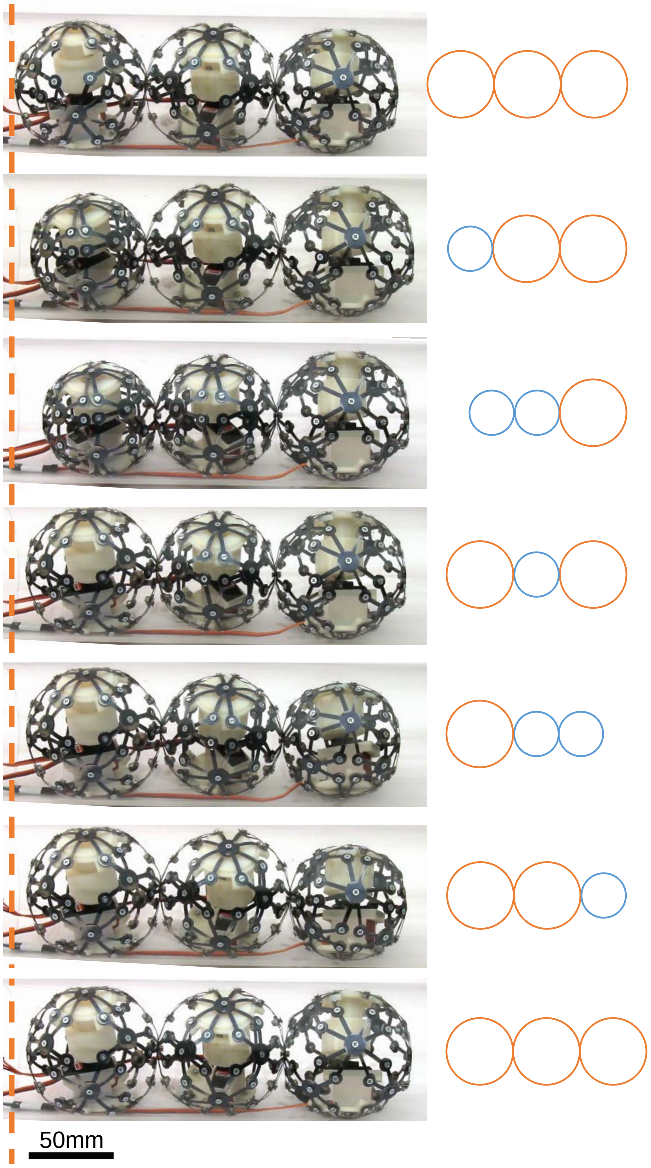

Fig. 5. Three auxetic cells form a tube crawling robot. The sequence pictured here can be used for vertical or horizontal tube crawling. The activated and expanded cells are represented by large orange circles, while the passive collapsed cells are represented by smaller blue circles. The robot depicted here is from a horizontal tube crawl

Although this crawling is significantly slower than desired, we do note that the robots' top speed is limited by the quality of 3D printed parts used, not by the motor or auxetic shell. This strongly suggests that future versions of our volumetric actuator should be made with stronger plastic components to allow for faster actuation and make the tube crawler more comparable to the soft pneumatic auxetic robot.

We also evaluated the maximum payload a single unit in a vertical tube could hold, giving a sense of how much load could be held against gravity. To measure this, we pulled on a single unit in the actuated open position within the tube, measuring the force applied via a force gauge. We found that a single unit could withstand a pull-down force of 9 N and a top-down push-down force of 11 N. Given that a single volumetric actuator weighs about 80 g, a single unit could theoretically haul 11 times its own weight.

The discrepancy between the pull-down and push-down force was surprising. Normally, we'd expect an auxetic structure to contract when pushed and expand when pulled, resulting in a lower force needed for push-down than for pull-down. Since we observed the opposite, this presents further evidence that the the servo motor can generate enough torque to prevent the auxetic deformation of the structure, turning it into a non-auxetic material.

VI. CONCLUSIONS AND FUTURE WORK

In this work we have introduced a new class of independent cellular volumetric actuators based on auxetic materials driven by servos. These actuators rely on antipodal rotations in point group auxetics. We have shown that both axial symmetric and polyhedral symmetric structures can produce counter-rotating antipodal points. Based on this work, we can conclude that the axial symmetric shearing auxetic frameworks are inferior to those with polyhedral symmetries for volumetric actuation applications. We believe this result will generalize to other axial symmetric auxetic structures.

We have been able to replicate the results of many soft fluid driven auxetic robots. Our actuator can be considered an electric version of the soft actuator described in [18] and was modular enough to replicate the tube crawling robot described in [16]. Given the results presented here and in [22], we can conclude that motor driven auxetics can be used in most or all applications where fluid driven auxetics have been used in the past. Although these actuators are currently limited by the need for external power and control, given the large voids in the closed state of the structure, it should be possible to embed power and control electronics within the actuators themselves.

Despite making actuators from two layers of non-oriented isometric auxetic shells, the actuator we produced are not isometric. We conclude that the act of connecting the antipodal points provides an orientation to the shell. While this was not desired, it does present an interesting future work direction as it begs further questions into how the orientation and distribution of these layers directly affect the global mechanical properties.

Furthermore, the servo driven nature of these actuators presents an interesting case for using these actuators as a variable stiffness material. By varying the torque generated by the servo, we can effectively vary the stiffness of the structure. In the future, this induced orientation and variable stiffness could be exploited to make interesting mechanical properties from combining many of these actuators. We believe these actuators provide an exciting new opportunity for robotics and material science.

ACKNOWLEDGMENTS

This work was completed with support from the Boeing Company and the National Science Foundation under grant #1830901 . LC was supported under the National Science Foundation Graduate Research Fellowship grant #1122374, the Paul & Daisy Soros Fellowship for New Americans, and the Fannie and John Hertz Foundation. This article solely reflects the opinions and conclusions of its authors and not that of its sponsors.

The authors would like to thank Robert MacCurdy, Austin Wang, Miles Dai, Edmund Williams, and Gregory Xie for their help in this research.

References

[1] B. Mosadegh, P. Polygerinos, C. Keplinger, S. Wennstedt, R. F. Shepherd, U. Gupta, J. Shim, K. Bertoldi, C. J. Walsh, and G. M. Whitesides, "Pneumatic networks for soft robotics that actuate rapidly," *Advanced functional materials*, vol. 24, no. 15, pp. 2163–2170, 2014.

[2] M. A. Robertson and J. Paik, "New soft robots really suck: Vacuum-powered systems empower diverse capabilities," *Science Robotics*, vol. 2, no. 9, p. eaan6357, 2017.

[3] S. Li, D. M. Vogt, D. Rus, and R. J. Wood, "Fluid-driven origami-inspired artificial muscles," *Proceedings of the National Academy of Sciences*, vol. 114, no. 50, pp. 13 132–13 137, 2017.

[4] S. Terryn, J. Brancart, D. Lefeber, G. Van Assche, and B. Vanderborght, "Self-healing soft pneumatic robots," *Sci. Robot.*, vol. 2, no. 9, 2017.

[5] R. V. Martinez, A. C. Glavan, C. Keplinger, A. I. Oyetibo, and G. M. Whitesides, "Soft actuators and robots that are resistant to mechanical damage," *Advanced Functional Materials*, vol. 24, no. 20, pp. 3003–3010, 2014.

[6] P.-S. Juo, *Concise dictionary of biomedicine and molecular biology*. Crc Press, 2001.

[7] G. K. Muday, "Auxins and tropisms," *Journal of plant growth regulation*, vol. 20, no. 3, pp. 226–243, 2001.

[8] J. Hiller and H. Lipson, "Automatic design and manufacture of soft robots," *IEEE Transactions on Robotics*, vol. 28, no. 2, pp. 457–466, 2012.

[9] N. Cheney, R. MacCurdy, J. Clune, and H. Lipson, "Unshackling evolution: evolving soft robots with multiple materials and a powerful generative encoding," *ACM SIGEVOlution*, vol. 7, no. 1, pp. 11–23, 2014.

[10] M. Joachimczak, R. Suzuki, and T. Arita, "Artificial metamorphosis: evolutionary design of transforming, soft-bodied robots," *Artificial life*, vol. 22, no. 3, pp. 271–298, 2016.

[11] J. I. Lipton, S. Angle, R. E. Banai, E. Peretz, and H. Lipson, "Electrically actuated hydraulic solids," *Advanced Engineering Materials*, vol. 18, no. 10, pp. 1710–1715, 2016.

[12] A. Miriyev, K. Stack, and H. Lipson, "Soft material for soft actuators," *Nature communications*, vol. 8, no. 1, p. 596, 2017.

[13] S. Ceron, A. Kurumunda, E. Garg, M. Kim, T. Yeku, and K. Pctersen, "Popcorn-driven robotic actuators," in *2018 IEEE International Conference on Robotics and Automation (ICRA)*. IEEE, 2018, pp. 1–6.

[14] D. Rus and M. Vona, "A physical implementation of the self-reconfiguring crystalline robot," in *Proceedings 2000 ICRA. Millennium Conference. IEEE International Conference on Robotics and Automation. Symposia Proceedings (Cat. No. 00CH37065)*, vol. 2. IEEE, 2000, pp. 1726–1733.

[15] J. W. Suh, S. B. Homans, and M. Yim, "Telecubes: Mechanical design of a module for self-reconfigurable robotics," in *Proceedings 2002 IEEE International Conference on Robotics and Automation (Cat. No. 02CH37292)*, vol. 4. IEEE, 2002, pp. 4095–4101.

[16] A. G. Mark, S. Palagi, T. Qiu, and P. Fischer, "Auxetic metamaterial simplifies soft robot design," in *2016 IEEE International Conference on Robotics and Automation (ICRA)*. Ieee, 2016, pp. 4951–4956.

[17] A. Sedal, M. Fisher, J. Bishop-Moser, A. Wineman, and S. Kota, "Auxetic sleeves for soft actuators with kinematically varied surfaces," in *2018 IEEE/RSJ International Conference on Intelligent Robots and Systems (IROS)*. IEEE, 2018, pp. 464–471.

[18] J. Shim, C. Perdigou, E. R. Chen, K. Bertoldi, and P. M. Reis, "Buckling-induced encapsulation of structured elastic shells under pressure," *Proceedings of the National Academy of Sciences*, vol. 109, no. 16, pp. 5978–5983, 2012.

[19] A. Lazarus and P. M. Reis, "Soft actuation of structured cylinders through auxetic behavior," *Advanced Engineering Materials*, vol. 17, no. 6, pp. 815–820, 2015.

[20] D. Yang, M. S. Verma, J.-H. So, B. Mosadegh, C. Keplinger, B. Lee, F. Khashai, E. Lossner, Z. Suo, and G. M. Whitesides, "Buckling pneumatic linear actuators inspired by muscle," *Advanced Materials Technologies*, vol. 1, no. 3, p. 1600055, 2016.

[21] D. Yang, B. Mosadegh, A. Ainla, B. Lee, F. Khashai, Z. Suo, K. Bertoldi, and G. M. Whitesides, "Buckling of elastomeric beams enables actuation of soft machines," *Advanced Materials*, vol. 27, no. 41, pp. 6323–6327, 2015.

[22] J. I. Lipton, R. MacCurdy, Z. Manchester, L. Chin, D. Cellucci, and D. Rus, "Handedness in shearing auxetics creates rigid and compliant structures," *Science*, vol. 360, no. 6389, pp. 632–635, 2018.

[23] L. Chin, J. Lipton, R. MacCurdy, J. Romanishin, C. Sharma, and D. Rus, "Compliant electric actuators based on handed shearing auxetics," in *2018 IEEE International Conference on Soft Robotics (RoboSoft)*. IEEE, 2018, pp. 100–107.

[24] C. Hoberman, "Reversibly expandable doubly-curved truss structure," July 24 1990, uS Patent 4,942,700.

[25] F. Kovács, T. Tarnai, P. Fowler, and S. Guest, "A class of expandable polyhedral structures," *International journal of solids and structures*, vol. 41, no. 3-4, pp. 1119–1137, 2004.